An Experimental Study for a High-resolution 3-D Imaging Algorithm with Linear Array for UWB Radars

Shouhei KIDERA, Yusuke KANI, Takuya SAKAMOTO and Toru SATO

Graduate School of Informatics, Kyoto University, Kyoto, 606-8501, Japan

Abstract— **Pulse radars with UWB signals are promising as a high-resolution imaging technique that can be used for a non-destructive measurement of surface details on reflector antennas and airplane. We previously proposed a fast 3-D imaging algorithm, SEABED, that utilizes a reversible transform between the time delay and the target boundary. However, data acquisition is time-consuming when obtaining a high-resolution image because it assumes a mono-static radar with 2-D scanning of an antenna. In this paper, we utilize linear array antennas and propose a fast and high-resolution imaging algorithm. We extend the reversible transform for mono-static radars to apply to bi-static radars to reduce the data acquisition time. The effectiveness of the proposed method is verified with numerical simulations and experiments.**

Index Terms — **UWB pulse radars, Fast and high-resolution imaging, BST, Bi-static radar, Linear array antennas**

I. INTRODUCTION

UWB pulse radars have a great potential for a high-resolution imaging that is suitable for a non-destructive measurement technique. This can be applied to detect the small surface defects on a reflector antenna and a fuselage of airplane. In addition, they are suitable for target positioning systems of rescue robots in dark smoke. These applications require real-time imaging. While various imaging algorithms for radars have been developed, they require intensive computation for target imaging [1-4]. To resolve this problem, we have proposed a fast 3-D imaging algorithm, SEABED, that utilizes a reversible transform BST (Boundary Scattering Transform) between the time delays and the target boundary [5-7]. This method accomplishes a fast and non-parametric imaging with the received data. However, it requires a long time for the data acquisition to obtain a high-resolution image, because it assumes 2-D scanning of an antenna as a mono-static radar. Thus, SEABED has a trade-off between the data acquisition time and the resolution of the estimated image.

In this paper, we propose a rapid and high-resolution imaging algorithm with linear array antennas to resolve this trade-off. The resolution of the image with the original SEABED is limited to an interval of array antennas because BST is applied only to mono-static radars. The interval of array antennas should be more than half of the center wavelength of the pulse to avoid the mutual couplings; this limits the resolution of SEABED images. In this paper, we extend BST to apply to bi-static radars and propose a high-resolution imaging algorithm. This method has been verified the effectiveness in terms of fast and high-
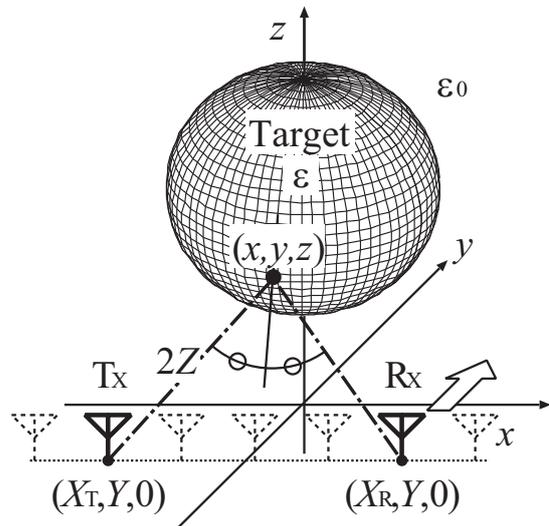

Fig. 1. System model.

resolution in numerical simulations[8]. Now, we investigate the performance evaluation of our proposed method with an experiment by utilizing UWB modules.

II. SYSTEM MODEL

The system model is shown in Fig. 1. We assume that the target has a clear boundary, which is expressed as a single-value function of x and y. We assume that the propagation speed of the radiowave is known and constant. A mono-cycle pulse is utilized as the transmitting current and, we assume the linear polarization in the direction of x axis. We locate omni-directional antennas with a fixed interval along x axis, and scan it along y axis on $z = 0$ plane.

R-space is defined as the real space, in which targets and antennas are located, and is expressed by the parameters (x, y, z). This space is also normalized by λ, which is the center wavelength of the transmitted pulse. We assume $z > 0$ for simplicity. The locations of the transmitting and receiving antennas are defined as $(x, y, z) = (X_{\mathrm{T}}, Y, 0)$ and $(X_{\mathrm{R}}, Y, 0)$, respectively. $s'(X_{\mathrm{T}}, X_{\mathrm{R}}, Y, Z')$ is defined as the received electric field. We also define Z' with time t and speed of the radio wave c as $Z' = \mathrm{c}t/2\lambda$. $s(X_{\mathrm{T}}, X_{\mathrm{R}}, Y, Z')$ is defined as the output of the matched filter with the transmitted waveform. We extract the significant peaks of $s(X_{\mathrm{T}}, X_{\mathrm{R}}, Y, Z')$ as Z for each $X_{\mathrm{T}}, X_{\mathrm{R}}$ and Y, and define the extracted surface as $(X_{\mathrm{T}}, X_{\mathrm{R}}, Y, Z)$, which is called a
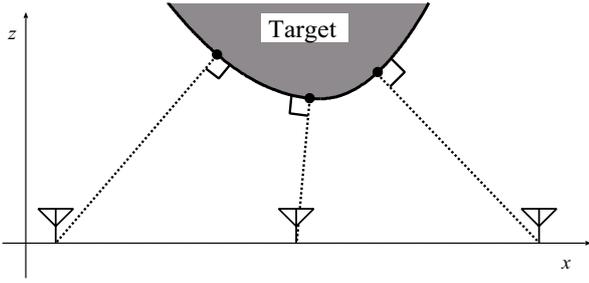
Fig. 2. Relationship between estimated points and antenna locations of the conventional model.
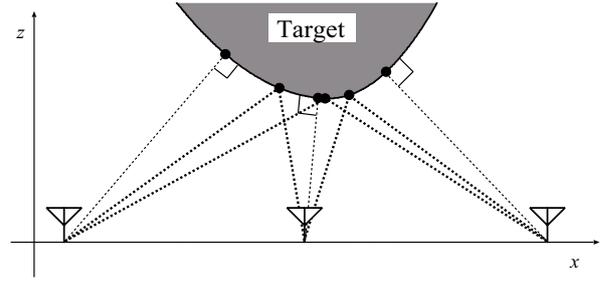

Fig. 3. Relationship between estimated points and antenna locations of the proposed model.

quasi wavefront. D-space is defined as the space expressed by (X_T, X_R, Y, Z). The transform from d-space to r-space corresponds to the imaging that we deal with in this paper.

III. Imaging Algorithm

A. Conventional Method

We have already developed a high-speed imaging algorithm as SEABED. This method utilizes a mono-static radar, and we define as $X = X_T = X_R$. It clarifies the existence of a reversible transform BST (Boundary Scattering Transform) between the target boundary (x, y, z) and the quasi wavefront (X, Y, Z) [7]. IBST (Inverse BST) is expressed as

$$\left. \begin{array}{rcl} x & = & X - ZZ_X \\ y & = & Y - ZZ_Y \\ z & = & Z\sqrt{1 - Z_X^2 - Z_Y^2} \end{array} \right\}, \quad (1)$$

where $Z_X = \partial Z/\partial X$ and $Z_Y = \partial Z/\partial Y$. This transform gives us a complete solution for the inverse problem. Although this method realizes a high-speed imaging, the resolution of the image is limited to the number of the antennas because it assumes a mono-static radar. Fig. 2 shows the relationship between the estimated points with this method and antenna locations in 2-D problem, for simplicity. As shown in Fig. 2, the estimated image has insufficient resolution around target edges. If we increase the number of scanning samples to enhance the resolution, data acquisition becomes time-intensive. Accordingly, there is a trade-off between the time taken to obtain the data and the resolution of the estimated image.

B. Proposed Method

To resolve the trade-off described in the previous section, we propose a fast and high-resolution imaging method with linear array antennas. First, we introduce a reversible transform BST for bi-static radars. We fix the interval of the transmitted and received antennas, and set it to $2d$. The center position of the two antennas is $x = (X_T + X_R)/2$, $y = Y$ and $z = 0$, and $X = (X_T + X_R)/2$

is defined. The scattering center on the target boundary is defined as (x, y, z). Z is the distance to the scattering point, where the law of reflection is satisfied. With this geometrical condition, (X, Y, Z) is expressed as

$$\left. \begin{array}{rcl} X & = & x + \frac{2z_x(z^2 + z^2 z_x^2 + d^2)}{z(1 - z_x^2 + z_y^2) + \sqrt{z^2(1 + z_x^2 + z_y^2)^2 + 4d^2 z_x^2}} \\ Y & = & y + zz_y \\ Z & = & \sqrt{z^2(1 + z_y^2) + zz_x(X - x) + d^2} \end{array} \right\}, \quad (2)$$

where $z_x = \partial z/\partial x$, $z_y = \partial z/\partial y$. We call this transform BBST (Bi-static BST). (x, y, z) is also expressed as

$$\left. \begin{array}{rcl} x & = & X - \frac{2Z^3 Z_X}{Z^2 - d^2 + \sqrt{(Z^2 - d^2)^2 + 4d^2 Z^2 Z_X{}^2}} \\ y & = & Y + Z_Y\{d^2(x - X)^2 - Z^4\}/Z^3 \\ z & = & \sqrt{Z^2 - d^2 - (y - Y)^2 - \frac{(Z^2 - d^2)(x - X)^2}{Z^2}} \end{array} \right\}. \quad (3)$$

We call this transform IBBST (Inverse BBST). IBBST is effective for real-time imaging as we can directly estimate the target boundary by using this transform with bi-static radars.

C. Procedure of the Proposed Method

We apply IBBST to the linear array antennas as described in the following procedures. We define the number of the antennas as N_X, and the interval of the array antennas as ΔX. First, $k = 0$ is set.

Step 1). Apply the matched filter to $s'(X_T, X_R, Y, Z')$ and obtain the output as $s(X_T, X_R, Y, Z')$.

Step 2). Extract the quasi wavefront as (X_T, X_R, Y, Z) by connecting the peaks of $s(X_T, X_R, Y, Z')$.

Step 3. Set $2d = k\Delta X$, and extract a cross section of the quasi wavefront as (X, Y, Z) where $X = (X_T + X_R)/2$ and $X_R = X_T + 2d$ hold.

Step 4). Apply IBBST to the extracted curve (X, Y, Z) and obtain a target image.

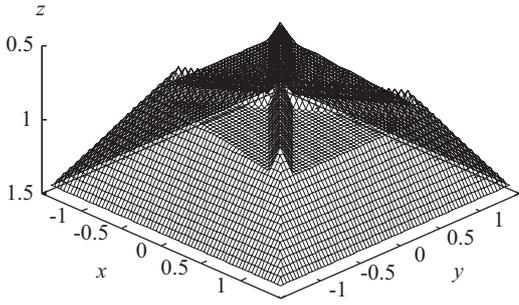Step 5). Set $k = k + 1$. If $k \leq N_X - 1$ holds, return to Step 3), otherwise complete the shape estimation.
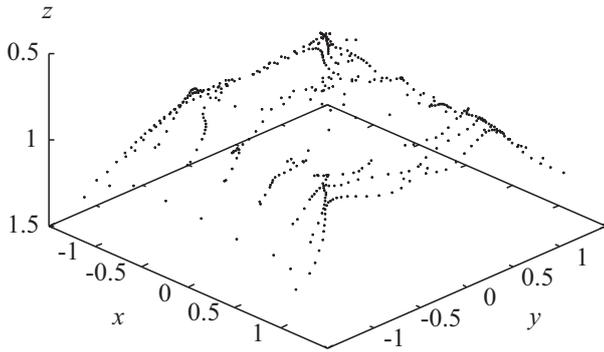
Fig. 4. Assumed target boundary.

Fig. 6. Estimated image with the proposed method.

Fig. 5. Estimated image with the conventional method.

Fig. 7. Linear array antennas and the target.

This method enables us to increase the estimated points to $N_X(N_X-1)/2$ by changing the parameter d for the x direction. Fig. 3 shows the relationship between the estimated points with the proposed method and antenna locations in 2-D problem. Each of the estimated points is located at a different point on the target surface because the scattered wave propagate along a different path as shown in Fig. 3. This means that we can enhance the resolution of the target image using just a small number of antennas.

IV. PERFORMANCE EVALUATION

A. Application Example with Numerical Simulations

We now consider examples of shape estimations with numerical simulations. The target shape is set as shown in Fig. 4. The linear array antenna is set for $-2.0\lambda \leq x \leq 2.0\lambda$, where each interval of the antennas is 0.4λ, and $N_X = 11$. We scan this array antenna for $-2.0\lambda \leq y \leq 2.0\lambda$, where the number of observations N_Y is 51. The received signals are calculated with FDTD method in a noiseless environment. Fig. 5 shows the estimated image with the conventional method, in which the total number of estimated points is 432. It is clear that the conventional method has insufficient resolution to express the target surface for the x direction, especially on the upper side of the target. This is because the number of estimated points for the x direction
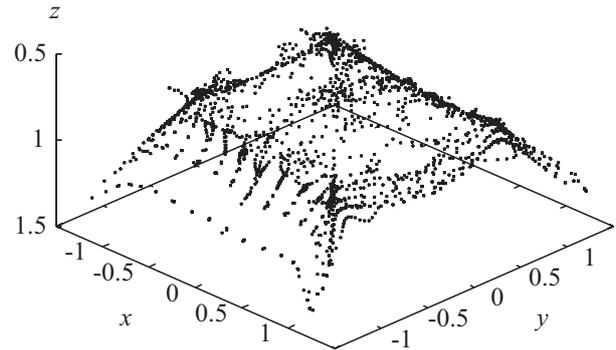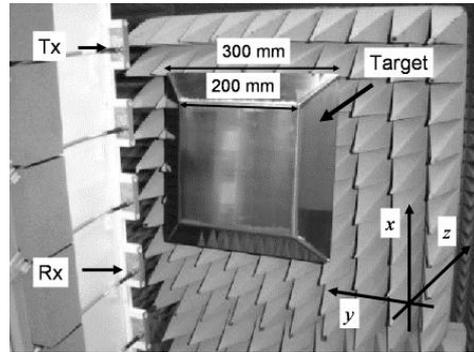
is limited to N_X. In contrast, Fig. 6 shows the estimated image with the proposed method, which achieves a higher resolution for the x direction. In this method, the total number of estimated points is 1920. These results verify that the proposed method has the advantage of providing a high-resolution image without the need to increase the number of antennas. However, the resolution of the image is distorted around the target edges. This is because deformation of the scattered waveform generates the errors in the quasi wavefront. It is our future task to enhance the accuracy around this region by compensating these distortions like the previous work[9], [10]. The computational time for imaging is within 30 msec with a single Xeon 3.2 GHz processor, which is sufficiently quick for real-time operations.

B. Application Example with Experiment

The performance with the experiment is evaluated as follows. Fig. 7 shows the arrangement of the linear array antennas and the target, and the coordinates used in the experiment. We utilize UWB signal with a center frequency of 3.2 GHz and a 10dB-bandwidth of 2.0 GHz. The antenna has an elliptic polarization whose ratio of the major axis to the minor one is about 17 dB, and the direction of the polarimetry is along x axis. The 3dB beam width
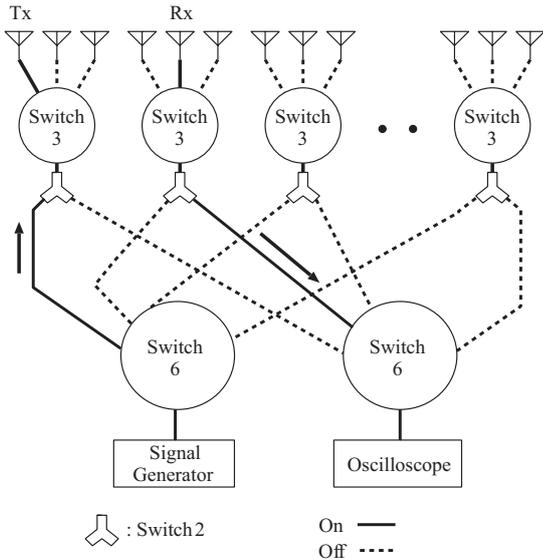
Fig. 8. Arrangement of high-frequency relays and antennas.

Fig. 9. True target boundary used in the experiment.

Fig. 10. Examples of the output of the matched filter ($X_{\mathrm{T}} = 100.0$mm, $X_{\mathrm{R}} = -200.0$mm).

of the antenna is about 90°. The linear array antennas are set in the vertical direction with 18 antennas. The interval is 100 mm, which corresponds to 1.1 center wavelength of the pulse. The array antennas are scanned along the y axis for -300 mm $\leq y \leq 300$ mm. The sampling interval is 10.0 mm, and $N_Y = 61$. The data are coherently averaged 256 times to enhance the S/N. We preliminarily measure the direct wave from the transmitting antenna without any targets, and eliminate this signal from the observed signals with a target in order to obtain the scattered waveform. We observe the transmitted waveform as the reflection from a large specular board, that is 1920 mm in hight and 1180 mm in width. We utilize the high-frequency relays as switches, where the isolation ratio of each relay is 50 dB, and the switching time is within 100 msec. We divide 18 antennas into 6 groups. To simplify the switching system, we do not select the transmitting and receiving antennas from the same group. Fig. 8 shows the arrangement of the relays and the antennas in the experiment.

We set a metallic hexahedral target made of stainless steel sheeting with a thickness of 3 mm. Fig. 9 shows the true target boundary. We utilize 11 antennas set for -500.0 mm $\leq x \leq 500.0$ mm. Fig. 10 shows the output of the matched filter in our experiment, where we set $X_{\mathrm{T}} = 100.0$ mm and $X_{\mathrm{R}} = -200.0$ mm. The S/N in the experiment is 32.0 dB, where we define the S/N as the ratio of peak instantaneous signal power to the averaged noise power after applying the matched filter. This also corresponds to the standard deviation $3.0 \times 10^{-3}\lambda$ of the Gaussian random error of the quasi wavefront [11]. The extracted quasi wavefront is smoothed with the Gaussian filter, whose correlation length is 0.2λ. Fig. 11 shows the
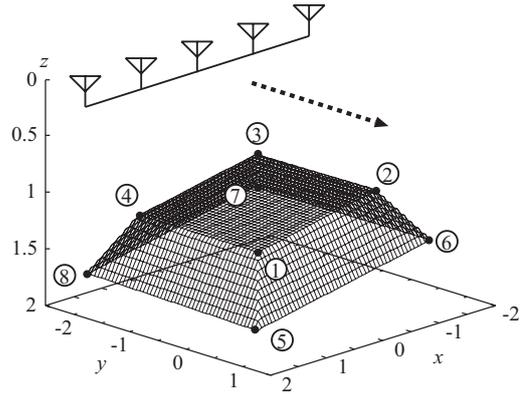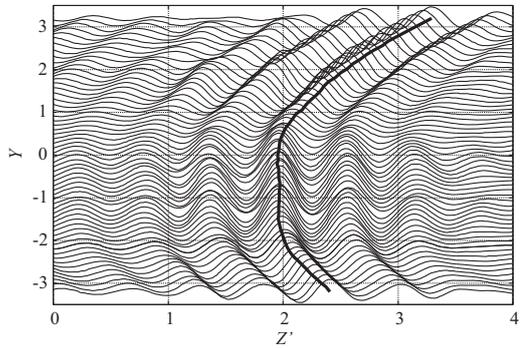
estimated image with the conventional method. The colors of the estimated points represent the estimation error, calculated as the distance to the true target boundary. The number of estimated points is 166. As shown in this figure, the image has an insufficient resolution in the x direction to locate the edges and surface details. Fig. 12 shows the estimated image with the proposed method. Our method obtains a higher-resolution image around the target edges and the surface details for the x direction compared to that shown in Fig. 11. The number of estimated points is 496. We quantitatively evaluate the accuracy of the two methods with an evaluation value ϵ that is defined as

$$\epsilon = \sqrt{\frac{1}{N}\sum_{i=0}^{N} \min_{\boldsymbol{x}} \|\boldsymbol{x} - \boldsymbol{x}_{\mathrm{e}}^i\|^2}, \qquad (4)$$

where $\boldsymbol{x}$ and $\boldsymbol{x}_{\mathrm{e}}^i$ express the location of the true target points and that of the estimated points, respectively. Values of ϵ with the conventional and proposed methods are $8.8325 \times 10^{-2}\lambda$ and $8.9174 \times 10^{-2}\lambda$, respectively. In addition, Fig. 13 shows the minimum error to the edge points of the target boundary. The numbers along the horizontal axis correspond to those of the target edges as shown in Fig. 9. Fig. 13 confirms that the proposed method is able
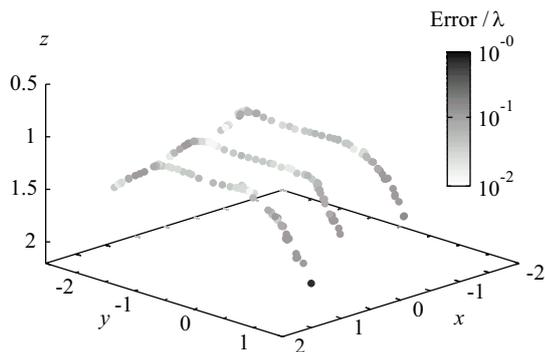
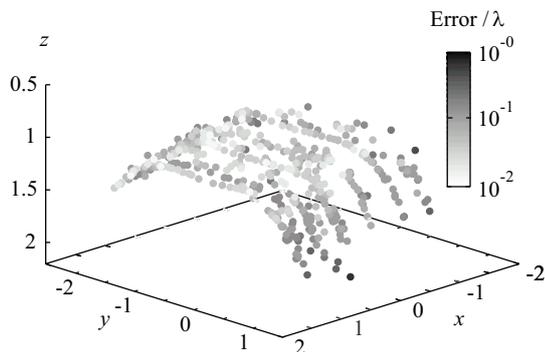Fig. 11. Estimated image with the conventional method in the experiment.

Fig. 12. Estimated image with the proposed method in the experiment.

to determine the edge locations more accurately compared to the conventional method. This is because the proposed method can increase the number of the estimated points. These results demonstrate that the proposed method is able to obtain a higher-resolution image in the real environment. It is confirmed that the time for data acquisition with array antennas is 5 times shorter than that of the conventional system, where the same resolution is assumed. The calculation time for each method with the received data is within 30 msec with a single Xeon 3.2 GHz processor.

The estimated accuracy of Fig. 12 deteriorates around the side of the target due to deformation of the scattered waveform. Namely, these deformations cause the errors of quasi wavefront because the matched filter with the transmitted waveform is applied. In addition, the estimated points diverge due to the noise. This is because the estimated image can be fluctuated with a random noise by the derivative operation of IBBST. Thus, data is required with higher SNR and SIR to enhance the robustness of the image.
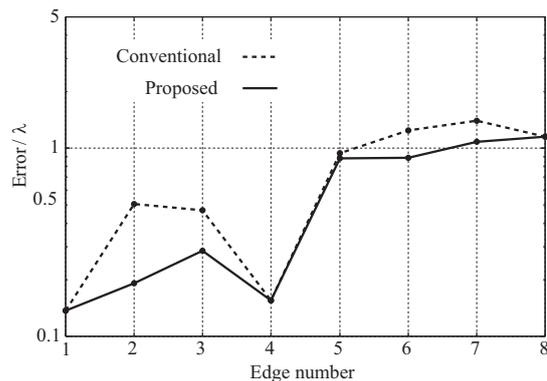

Fig. 13. Estimated errors for the target edges.

V. Conclusion

We proposed a fast and high-resolution imaging algorithm with linear array antennas. The reversible transform BBST for bi-static radars was applied to the array systems. We investigated the performance of the proposed algorithm in numerical simulations and an experiment that involved the linear array antennas. We confirmed that the proposed method improves the resolution of the image around the edges in the real environment without increasing the number of antennas. It is our future task to enhance the accuracy around the edges by applying the shape and waveform estimations.

Acknowledgment

References

[1] C. Chiu, C. Li, and W. Chan, "Image reconstruction of a buried conductor by the genetic algorithm," *IEICE Trans. Electron.*, vol. E84-C, no. 12, pp. 1946–1951, 2001.

[2] T. Takenaka, H. Jia, and T. Tanaka, "Microwave imaging of an anisotropic cylindrical object by a forward-backward time-stepping method," *IEICE Trans. Electron.*, vol. E84-C, no. pp. 1910–1916, 2001.

[3] T. Sato, K. Takeda, T. Nagamatsu, T. Wakayama, I. Kimura and T. Shinbo, "Automatic signal processing of front monitor radar for tunneling machines," *IEEE Trans. Geosci. Remote Sens.*, vol.35, no.2, pp.354-359, 1997.

[4] T. Sato, T. Wakayama, and K. Takemura, "An imaging algorithm of objects embedded in a lossy dispersive medium for sub-surface radar data processing," *IEEE Trans. Geosci. Remote Sens.*, vol.38, no.1, pp.296–303, 2000.

[5] T. Sakamoto and T. Sato, "A target shape estimation algorithm for pulse radar systems based on boundary scattering transform," *IEICE Trans. Commun.*, vol.E87-B, no.5, pp. 1357–1365, 2004.

[6] T. Sakamoto and T. Sato, "A phase compensation algorithm for high-resolution pulse radar systems," *IEICE Trans. Commun.*, vol.E87-B, no.6, pp. 1631–1638, 2004.

[7] T. Sakamoto, "A fast algorithm for 3-dimensional imaging with UWB pulse radar systems," *IEICE Trans. Commun.*, vol.E90-B, no.3, 2007 (in press).

[8] S. Kidera, T. Sakamoto and T. Sato, "An high-resolution 3-D imaging algorithm with linear array antennas for UWB pulse

radars." IEEE AP-S Internatinal Symposium, URSI National Radio Science Meeting, AMEREM Meeting, pp. 1057–1060, Jul, 2006.

[9] S. Kidera, T. Sakamoto, T. Sato, and S. Sugino, "An accurate imaging algorithm with scattered waveform estimation for UWB pulse radars", *IEICE Trans. Commun.*, vol.E89-B, no. 9, pp. 2588–2595, Sep, 2006.

[10] S. Kidera, T. Sakamoto, and T. Sato, "A robust and high-resolution imaging algorithm with waveform estimation for UWB pulse radars", *IEICE Trans. Commun.*, vol.E90-B, 2007 (in press).

[11] T. Sakamoto, "A 2-D image stabilization algorithm for UWB pulse radars with fractional boundary scattering transform," *IEICE Trans. Commun.*, vol.E90-B, no. 1, pp. 131–139, Jan, 2007.